

NEW EXTENDED RANGE WAC TiO₂ MAP OF THE MOON. H. Sato¹, B. Hapke², M. S. Robinson³, ¹Japan Aerospace Exploration Agency, 3-1-1 Yoshinodai, Chuo-ku, Sagami-hara, Kanagawa, Japan (sato.hiroyuki@jaxa.jp), ²University of Pittsburgh, Pittsburgh, PA, ³Arizona State University, Tempe, AZ.

Introduction: Accurate knowledge of the distribution and the abundance of TiO₂ of the lunar surface is key to understanding the magmatic history and thermal evolution of the Moon. TiO₂ abundance maps were derived by various studies using multiple remote-sensing datasets. The UV sensitivity of the Lunar Reconnaissance Orbiter Wide Angle Camera (WAC) enables quantification of the unique spectral shape of ilmenite that increases toward shorter wavelengths from visible to UV, whereas reflectance for other major lunar silicate minerals decreases into the UV. The WAC 321/415 nm ratio derived TiO₂ map [1] was sensitive down to TiO₂ abundances of 2 wt% (corresponds to the dominance of ilmenite in the total TiO₂ content). Below 2 wt% range for the WAC TiO₂ map, a new algorithm was proposed by [2,3]. It utilizes the 566/689 nm ratio that correlates with the content of pyroxene, the other TiO₂ bearing mineral. The algorithm is valid only for mature soils; for immature soils it gives a lower limit. Based on this new algorithm, here we created a new merged WAC TiO₂ map with no limit of the valid range, and we compared it with two pre-existing TiO₂ maps.

Methodology: We used the WAC seven color semi-global mosaic created by [4] (400 m/pixel at the equator, 70°S to 70°N in latitude). The new TiO₂ algorithm [2,3] first calculates two TiO₂ values:

$$\text{TiO}_2(566/689) = 34.48 - 41.49 * r(566/689)$$

$$\text{TiO}_2(321/415) = 169.8 * r(321/415) - 121.9$$

where $r(566/689)$ and $r(321/415)$ correspond to the I/F ratio of 566 nm over 689 nm and 321 nm over 415 nm, respectively. Then the final TiO₂ values (hereafter called WACTiO₂) are derived by the following condition:

$$\text{TiO}_2 = \begin{cases} \text{TiO}_2(321/415), & \text{if } \text{TiO}_2(321/415) > 3 \\ \text{TiO}_2(566/689), & \text{otherwise} \end{cases}$$

$$\text{TiO}_2 = 0, \text{ if } \text{TiO}_2 < 0$$

We compared the new WACTiO₂ with pre-existing TiO₂ maps derived from the Clementine UVVIS 415 and 750 nm bands (200 m/pixel) [5] (hereafter called CLMTiO₂) and the Lunar Prospector Gamma-Ray Spectrometer (GRS) (1 pixel/degree) [6,7] (hereafter called LPTiO₂).

Results: First, we examined the incompatible regions with the new TiO₂ algorithm [2,3]. From the scatter plot of TiO₂(321/415) vs. TiO₂(566/689) (Fig. 1), we defined the regions from R1 to R4. R2 and R4 are the incompatible regions where TiO₂(566/689) is higher than TiO₂(321/415) and lower than 0 wt%,

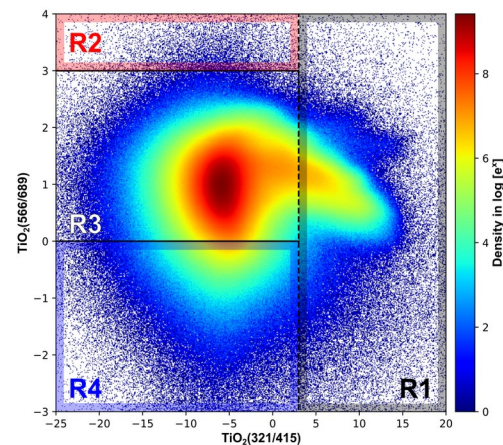


Figure 1. Density plot of TiO₂(321/415) vs TiO₂(566/689) for the whole area of WAC semi-global mosaic (70°S to 70°N). R# indicates the region number.

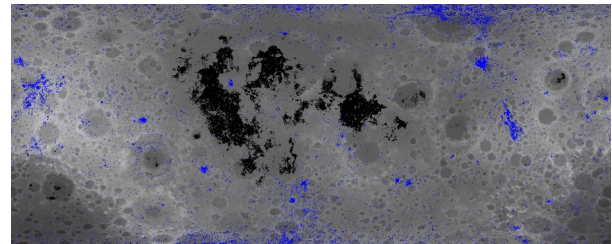


Figure 2. Spatial distribution of the R1 (black), R2 (red) and R4 (blue) in Fig. 1.

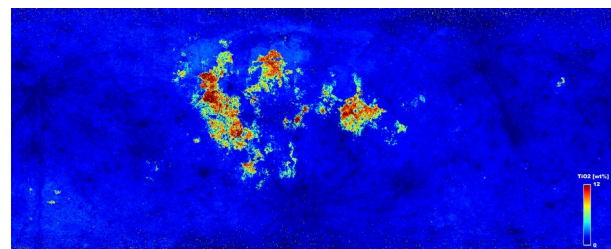


Figure 3. WACTiO₂ map based on the algorithm proposed by [2,3]. The spatial extent is from 180°W to 180°E, 70°S to 70°N.

respectively. In a map view (Fig. 2), R2 has less than 0.04% of areal fraction and is dominantly located in abnormal pixels such as shadows in high latitudes. Thus the R2 is likely caused by the artifacts.

The R4 is mainly located on immature highland ejecta, dominated by anorthositic materials [8] with TiO₂ values close to zero. Since the immature soil is not covered in the new algorithm [2,3] and can have a lower limit, negative values in the R4 are not surprising. The semi-global view of the new WACTiO₂ map (Fig. 3) has no noticeable offset at the 3 wt% transition.

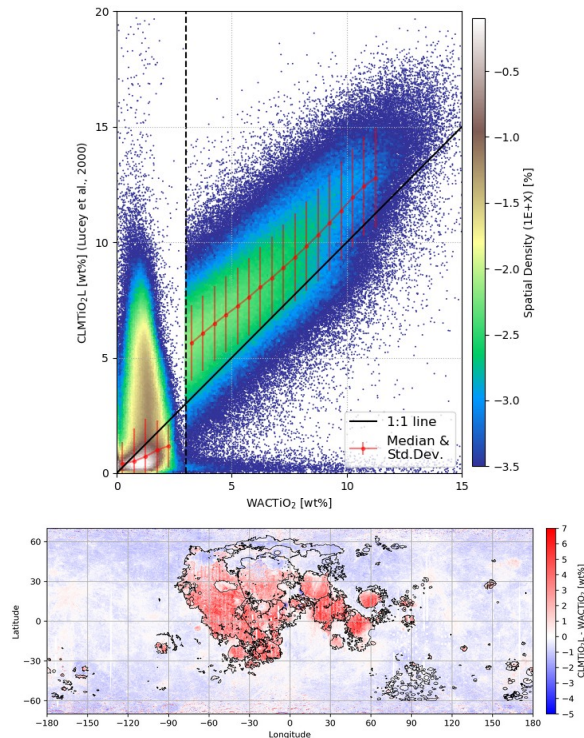


Figure 4. Density plot of CLMTiO₂ vs. WACTiO₂ (top) and difference map of CLMTiO₂ - WACTiO₂ (bottom). Bin size of the errorbar is 0.5 wt%. The mare boundaries are outlined by black line.

Compared to the CLMTiO₂, the WACTiO₂ is consistently lower (2.5 wt% on average; Fig. 4 top) above 3 wt% transition and is higher (up to twice on average) below 3 wt% transition, respectively. In the difference map (Fig. 4 bottom), the maria are dominantly red (= CLMTiO₂ > WACTiO₂) except Mare Frigoris and northern portions of Imbrium and Procellarum. In the highlands, mature regions are typically blue (= CLMTiO₂ < WACTiO₂), and the immature ejecta (set WACTiO₂ = 0 wt%) are light red.

The difference between the LPTiO₂ and WACTiO₂ is small (-0.1 wt% on average with $\sigma = 0.5$ wt%, Fig. 5 top), which is likely within the measurement errors of LP. The difference map (Fig. 5 bottom) shows locally red regions (= LPTiO₂ > WACTiO₂; up to +6 wt%) near Kepler and Aristarchus craters. A similar trend was also found in [1], possibly related to the sensible depth of GRS (~30 cm [9]) and the WAC (a few millimeters [10]). Immature highland ejecta are relatively red, but boundaries are not as sharp in Fig. 4 (bottom), likely due to the resolution effects. The difference in the highlands is -0.4 wt% on average, with $\sigma = 0.7$ wt%. For the mature highland surfaces, difference is greater (> -2 wt%), which is consistent trend as seen in Fig. 4.

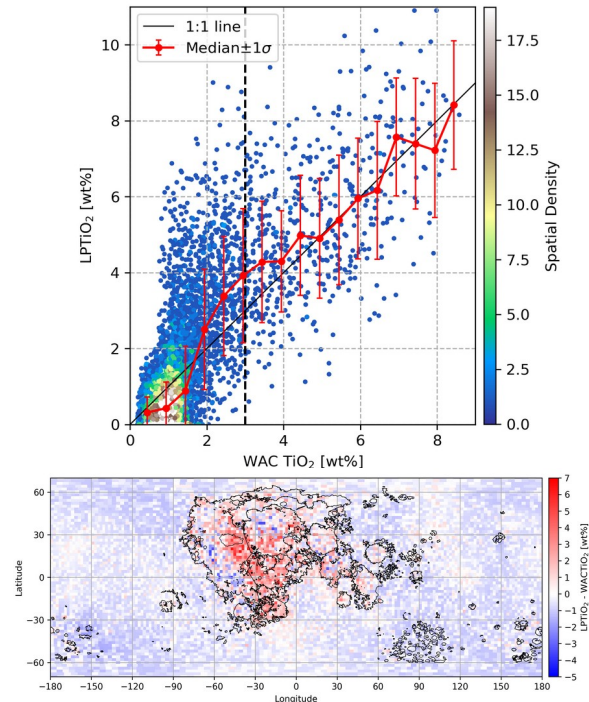


Figure 5. Density plot of LPTiO₂ vs. WACTiO₂ (top) and difference map of LPTiO₂ - WACTiO₂ (bottom). Bin size of the errorbar is 0.5 wt%.

Discussion: The sharp discontinuity of WACTiO₂ in Fig. 4 (top) corresponds to the transition of TiO₂(321/415) and TiO₂(566/689). The cause of this discontinuity is unknown. More local study along the 3 wt% transition boundaries in the WACTiO₂ map will help to clarify the cause and possibly improve the current algorithm.

The blue shift in Mare Frigoris and northern portions of Imbrium and Procellarum from the other red maria located in the lower latitudes in Fig. 4 (bottom) is not clear in Fig. 5 (bottom). This trend possibly corresponds to a latitudinal artifact in the CLMTiO₂.

Conclusion: The new WACTiO₂ based on the new algorithm has more relative offsets with the CLMTiO₂ than the LPTiO₂. More low-TiO₂ samples from the highlands (and the maria) are required for more accurate estimates of spectral reflectance for low-TiO₂ abundance, particularly in 0-1.5 wt% range.

References: [1] Sato et al. (2017) *Icarus* 296, 216-238. [2] Hapke et al. (2019) *Icarus* 321, 141-147. [3] Hapke et al. (2019) *Icarus*, in press. [4] Sato et al. (2014) *JGR-Planets*, 119, 1775-1805. [5] Lucey et al. (2000) *JGR*, 105 (E8), 20297-20305. [6] Elphic et al. (2000) *JGR-Planets*, 107 (E4), 5024. [7] Prettyman et al. (2006) *JGR*, 111 (E12), E12007. [8] Ohtake et al. (2009) *Nature*, 461 (7261), 236-40. [9] Lawrence, et al. (2002) *JGR* 107 (E12), 5130. [10] Hapke Hapke (2012) Cambridge University Press, New York.